SIGNAL ANALYSIS OF FIBER-OPTIC BIOSENSOR FOR THE DETECTION OF ORGANOPHOSPHORUS COMPOUNDS IN THE CONTAMINATED WATER

Jeong-Woo Choi[†], Junhong Min and Won-Hong Lee

Department of Chemical Engineering, Sogang University, C.P.O.Box 1142, Seoul, Korea

Abstract – The fiber-optic biosensor consisted of tubular enzyme reactor and two sensing parts was developed for the detection of organophosphorus compounds in a contaminated water. The organophosphorus compounds was measured by acetylcholinesterase entrapped by Ca-alginate gel on a silicon tube. The litmus dye was used as the indicator of color change due to the inhibition of organophosphorus compounds on the acetylcholinesterase. Transmittance change of light at the input and output parts of tubular enzyme reactor was detected. The biosensor has the linear analytical range of 0-1.0 ppm with response time of 5 minutes. The proposed kinetics for irreversible inhibition of organophosphorus compounds on AChE agreed well with the experimental data. The theoretical model of diffusion and reaction in enzyme membrane was presented to analyze the response of sensor signal. Based on the simulation results using the model, the optimal amount of enzyme loaded and substrate was obtained as 80 μg and 6 mM, respectively.

INTRODUCTION

Organophosphorus compounds which have been used as commercial pesticides and potential nerve toxins for military purposes have become increasingly important in recent years because these block the active site of nerve enzyme by nucleophilic attack [Alfthan et al., 1989]. Since the organophosphorus compounds are widely used in the farm for the plant protection purposes, rapid and simple detection of the contamination of ground water is required in water supplies [Klaimer et al., 1993; Leon-Gonzalez and Townshend, 1990; Wittmann and Schmid, 1993].

Fiber-optic sensor has many advantages compared with the other sensor types due to its capability of remote and multiple sensing [Abdel-Latif and Guidbault, 1990]. Also the fiber-optic sensor is not interfered by the electric field and is easy to miniaturize, which can lead to the development of very small, light and flexible sensor. Fiber-optic biosensor is the emerging technology that incorporates the sophisticated biological and optical components to analyze the specific components with high selectivity and sensitivity [Abdel-Latif and Guidbault, 1990; Carome et al., 1993].

Biosensors to detect the organophosphorus compounds have been developed [Dumschat et al., 1991; Skladal, 1991; Takruni et al., 1993; Wolfbeis and Koller, 1989]. Detection principle of these sensors is usually based on the inhibition of organophosphorus compounds on acetylcholinesterase (AChE), which is a hydrolyze enzyme with narrow specificity for acetylcholine and related compounds in nerve tissue. Absorbance change of product generated from the enzyme reaction in the packed bed reactor was used as the determination of the amount of organo-

phosphorus compounds [Trettnak et al., 1993]. The chromogenic synthetic enzyme substrate was used for the change of color formation in their report. But the sensor signal becomes inaccurate due to the detection of only absorbance change of product if the absorbance of the impurities was same as that of the product in the sample solution. Also the fluctuation of sensor signal could not be compensated because the reference signal was not detected. And the systematic analysis of the biosensor has not been reported in spite of its importance of the design of reaction part and operation.

In this study, a fiber-optic biosensor was developed with two sensing parts (the reference and indicator signal detection) and the tubular enzyme reactor. The litmus dye was used as the substrate for the color change. The AChE was immobilized at the inner wall of tube by Ca-alginate gel. To get the accurate sensor signal, the simultaneous detection of reference signal (absorbance change of substrate) and indicator signal (product after enzyme reaction) was done. The enzyme kinetics for the inhibition of organophosphorus compound on AChE and the model for tubular enzyme reactor were proposed to analyze the effects of operating and design parameters on sensor signal.

MATERIALS AND METHODS

1. Materials

Acetylcholinesterase (EC 3.1.1.7: V-S, from electric eel) with a specific activity of 1000U/mg, Paraoxon, m-nitrophenol and acetylthiocholine iodide were obtained from Sigma Chemical Company (St. Louis). The sensitive dye, litmus was supplied by BDH laboratory (Broom Rd poore, England).

2. Kinetic Experiment

Since AChE hydrolyzed acetylthiocholin to thiocholin and acetic acid, AChE activity could be measured by color change of

---

[†]To whom correspondence should be addressed.

the acid-base indicator, m-nitrophenol, at 400-440 nm due to the formation of acetic acid. To investigate the inhibition kinetics, various concentration of Paraoxon, used as an inhibitor, were added to solution of AChE and acetylthiocholin, and then absorbance change at 420 nm was measured by UV spectrophotometer (Shimadzu, Japan).

3. Enzyme Immobilization

AChE was immobilized on the inner wall of silicon tube (6 mm I.D and 6 cm length) using gelation of sodium alginate. The sodium alginate solution (1.5 % w/w) containing AChE (40 U/mg of 0.1 M potassium phosphate buffer (pH 7.0)) was prepared and flowed into the silicon tube in order to produce enzyme layer with nearly uniform thickness. Then the tube was placed in $CaCl_2$ solution (1.5 % w/w) for 20 min and the gel was formed on the inner surface of the tube due to ion exchange between Na^+ of sodium alginate and Ca^{++} of $CaCl_2$. The silicon tube with immobilized enzyme was stored in $CaCl_2$ solution (0.5 % w/w).

4. Construction of Fiber-Optic Biosensor

The experimental set-up was schematically shown in Fig. 1. The three solutions (distilled water, substrate solution of litmus and acetylthiocholin iodide, analyte solution) were prepared. Substrate solution and distilled water were mixed and flowed into tubular enzyme reactor via peristaltic pump at first. After enzyme reaction reached to the steady state, the distilled water was exchanged with analyte solution which contained various concentration of Paraoxon. The mixing ratio was 1:1 (v:v) for the substrate solution and distilled water or analyte solution.

Light emitting from the He-Ne laser (633 nm) was guided through two optical fiber lines to input and output parts of enzyme reactor. Transmitted light at two parts were guided through the opposite two fibers and then conveyed to two phototransis-
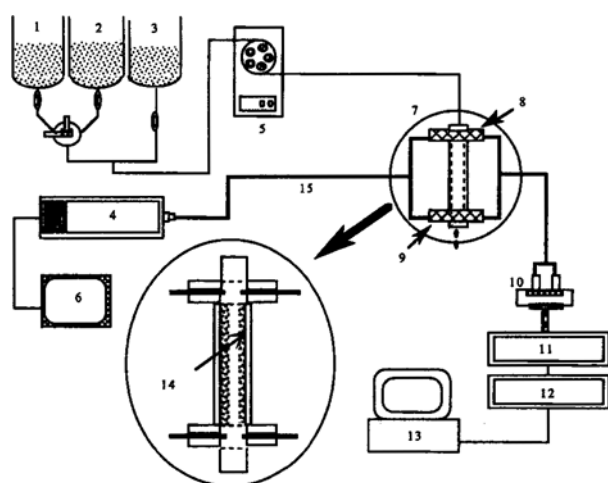

Fig. 1. The configuration of fiber-optic biosensor system.

1. Analyte reservoir	9. Indicator probe
2. Distilled water reservoir	10. Phototransistor
3. Dye and substrate reservoir	11. Amplifier
4. He-Ne laser	12. A/D converter
5. Peristaltic pump	13. Computer
6. Power supply	14. Enzyme layer
7. Reactor	15. Optical fiber
8. Reference probe	

tors, detectors. The detectors converted the optical signal into the electrical signal in order to obtain a quantitative value related to analyte concentration.

5. Signal Analysis

The reference and indicator signals were measured simultaneously at the input and output part of enzyme reactor, respectively. Indicator signal was corrected by Eq. (1). The reaction period was defined as period that substrate and distilled water flowed in the enzyme reactor without the inhibitor. The perturbation of signal was calculated based on the fluctuation of the reference signal.

$$\vartheta' = \vartheta + \psi - \vartheta_{rxn} \tag{1}$$

where, ϑ': The corrected signal
  ϑ: The indicator signal
  ψ: The perturbation
  ϑ_{rxn}: The indicator signal at reaction period

MODEL

To analyze the sensor signal, the mathematical model for tubular biosensor constructed with the combination of enzyme reaction kinetics and transport phenomena in the reactor is needed. Effects of the operating and design parameters on performances of biosensor such as detection range and response time can be simulated based on the model.

1. Enzyme Reaction Kinetics

The enzyme, AChE, has the following characteristics.

(1) Organophosphorus compounds inhibit AChE irreversibly [Alfthan et al., 1989].

(2) The inhibition is very fast compared with reaction of substrate.

(3) After inhibition step, the amount of inactivated enzyme is identical to that of inhibitor used.

Based on the above characteristics, irreversible inhibition scheme was proposed as shown in Fig. 2. The irreversible inhibition kinetics was obtained from the above inhibition scheme using quasi-steady state approximation.

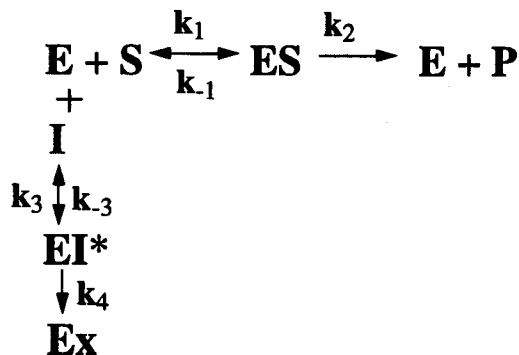$$V_P = \frac{V'_{max}\,[S]}{K'_m + [S]} \tag{2}$$

where,

Fig. 2. The enzyme inhibition scheme.
  E: Enzyme, I: Inhibitor, S: Substrate, P: Product, EI*: Excited complex, Ex: Inativated Enzyme

$$V_{max} = k_2 E_o \tag{3}$$

$$V'_{max} = V_{max} - k_2 (I_o - [I]) \tag{4}$$

$$k_m = (k_{-1} + k_2)/k_1 \tag{5}$$

$$K'_m = k_m (1 + [I]/k_I) \tag{6}$$

$$k_I = (k_4 + k_{-3})/k_3 \tag{7}$$

E_o is the amount of enzyme loaded in the alginate gel and I_o is the initial analyte concentration.

2. Model for Tubular Enzyme Reactor

The physical system and the associated notation are depicted in Fig. 3. Substrate and analyte are flowed into the annulus created by concentric active surface. The curvature of tube was ignored for the sake of simplicity since inside diameter of tube can be ignored compared with the tube length. In the mathematical analysis, it was used that substrate and analyte were flowed between two parallel plates. The followings occurred typically in the tubular enzyme reactor used. Enzyme was homogeneously immobilized on the wall side and irreversible reaction occurred only in the enzyme layer. The substrate was diffused into the immobilized enzyme layer, and then the product formed was diffused from enzyme layer to bulk phase. After the reaction period, the inhibitor was also drawn. Then, the product was reduced because the immobilized enzyme was inactivated. All reactants and product with diffusion coefficient, D_i, were diffused in the radial direction and were flowed in the axial direction in bulk phase. In the enzyme layer, the diffusions of reactants and product with D_{ei} in the radial direction were occurred.

The reactor part of biosensor could be described by the following set of governing equations.

In the bulk phase

$$\frac{\partial C_i}{\partial t} = -v \frac{\partial C_i}{\partial x} + D_i \frac{\partial^2 C_i}{\partial y^2} \tag{8}$$

In the enzyme layer

$$\frac{\partial C_{ei}}{\partial t} = D_{ei} \frac{\partial^2 C_{ei}}{\partial y^2} + V_i \tag{9}$$

The reaction term were expressed as follows.

$$V_1 = -\frac{V'_{max}[C_{e1}]}{K'_m + [C_{e1}]} \tag{10}$$

$$V_2 = -V_1 \tag{11}$$

$$V_2 = K_H V_1 \frac{[C_{e3}]}{[C_{e1}]} \tag{12}$$

where, $K_H = (k_{-1} + k_2) k_3 k_4 / (k_3 + k_4) k_1 k_2$ \hfill (13)

The subscript i could be correspond to acetylthiocholin iodide (i=1), acetic acid (i=2) and paraoxon (i=3). C_i and C_{ei} was local, time dependent concentration of the compounds in the bulk and enzyme phase of a reactor volume and v was the constant velocity of reactants and product. V_i was the reaction rate of i component.

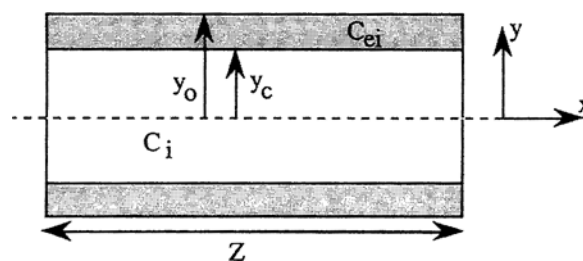The appropriate initial and boundary conditions for two phases

Fig. 3. The schematic diagram of an tubular reactor.
C_i: the concentration in the bulk phase, C_{ei}: the concentration in the enzyme phase, y: the radial direction, x: the axial direction, y_o: the radius of tubular enzyme reactor, y_c: the distance from the center of tubular enzyme reactor to enzyme layer, z: total length of tubular enzyme reactor.

were written as follows.

I.C. : $C_i = 0$, $\quad C_{ei} = 0$ $\quad$ for i=1, 2, 3

B.C.1 : $\left. \left| \frac{\partial C_i}{\partial y} \right| \right|_{y=0} = 0$

$C_i = C_{io}$, $\quad C_{ei} = 0$ $\quad$ for x=0

B.C.2 : $\left. \left| \frac{\partial C_{ei}}{\partial y} \right| \right|_{y=y_o} = 0$

B.C.3 : $\left. D_i \left| \frac{\partial C_i}{\partial y} \right| \right|_{y=y_c^+} = \left. D_{ei} \left| \frac{\partial C_{ei}}{\partial y} \right| \right|_{y=y_c^-}$

Where, the y_c^+ and y_c^- were the position maginally lower and higher than the interface position between bulk phase and enzyme layer.

The following dimensionless groups were introduced to transform the above governing equations into the dimensionless form.

$$\theta = \frac{t}{\bar{t}} \qquad \phi_i = \frac{C_i}{C_{io}} \qquad \phi_{ei} = \frac{C_{ei}}{C_{io}} \tag{14}$$

$$\xi = \frac{y}{y_2} \qquad \zeta = \frac{z}{L} \tag{15}$$

Eqs. (8)-(13) and conditions are thus reduced to

$$\frac{\partial \phi_i}{\partial \theta} = -\alpha \frac{\partial \phi_i}{\partial \zeta} + \beta_i \frac{\partial^2 \phi_i}{\partial \xi^2} \tag{16}$$

$$\frac{\partial \phi_{ei}}{\partial \theta} = -\gamma_i \frac{\partial^2 \phi_{ei}}{\partial \xi^2} + \Gamma_i \tag{17}$$

where Γ_i were expressed as,

$$\Gamma_1 = -\frac{\omega[\phi_{e1}]}{\kappa + [\phi_{e1}]} \tag{18}$$

$$\Gamma_2 = -\Gamma_1 \tag{19}$$

$$\Gamma_2 = K_H \Gamma_1 = \frac{[\phi_{e3}]}{[\phi_{e1}]} \tag{20}$$

I.C.: $\phi_i(\theta = 0, \xi, \zeta) = 0$, $\quad \phi_{ei}(\theta = 0, \xi, \zeta) = 0$ $\quad$ for i=1, 2, 3

B.C.1 : $\left. \dfrac{\partial\phi_i}{\partial\xi} \right|_{\zeta=0} = 0$

$\phi_i = 1$ and $\phi_{ei} = 0$ for $\zeta = 0$

B.C.2 : $\left. \dfrac{\partial\phi_{ei}}{\partial\xi} \right|_{\zeta=\zeta_c} = 0$

B.C.3 : $\left. \dfrac{\partial\phi_i}{\partial\xi} \right|_{\zeta=\zeta_c^+} = \eta_i \left. \dfrac{\partial\phi_{ei}}{\partial\xi} \right|_{\zeta=\zeta_c^-}$

while parameters in the above equations defined as

$$\alpha = \frac{v\bar{t}}{L} \qquad \beta_i = \frac{D_i \bar{t}}{y_c^2} \qquad \gamma_i = \frac{D_{e,i}\bar{t}}{y_c^2}$$

$$\Gamma_i = \frac{V_i \bar{t}}{C_{io}} \qquad \omega = \frac{V'_{max}\bar{t}}{C_{io}} \qquad \kappa = \frac{k_m}{C_{1o}} \qquad \eta_i = \frac{D_{ei}}{D_i} \qquad (21)$$

3. Numerical Technique

These equations may be solved using the method of collocation [Villadsen and Michelsen, 1978].

For the concentration of i component in bulk phase,

$$\frac{\partial\phi_{i,jk}}{\partial\zeta} = \sum_{l=1}^{N} A_{kl}\,\phi_{i,jl} \qquad (22)$$

$$\frac{\partial\phi_{i,jk}}{\partial\xi} = \sum_{p=1}^{M} B_{jp}\,\phi_{i,pk}, \qquad \frac{\partial^2\phi_{i,jk}}{\partial\xi^2} = \sum_{q=1}^{M} C_{jq}\,\phi_{i,qk} \qquad (23)$$

approximations can be made to the corresponding derivatives at the location ζ_i that are the roots of an Lth-order polynomial and at the location ξ_i that are the roots of an Mth-order polynomial. The semidiscretization elements A_{kl} and B_{jp} used to approximate the first derivatives, and C_{jp} used to approximate the second derivatives, depend on particular polynomial used.

For the concentration of i component in enzyme phase,

$$\frac{\partial\phi_{ei,hk}}{\partial\xi} = \sum_{r=1}^{L} D_{jr}\,\phi_{ei,rk}, \qquad \frac{\partial^2\phi_{ei,hk}}{\partial\xi^2} = \sum_{s=1}^{L} E_{js}\,\phi_{ei,sk} \qquad (24)$$

approximations can be able to the corresponding derivatives at the location ξ_i that are the roots of an Lth-order polynomial. The semidiscretization elements D_{jr} and E_{ij} used to approximate the first and second derivatives, respectively, depend on particular polynomial used.

The evaluation of these elements (A_{kl}, B_{jl}, C_{jq}, D_{jr}, E_{sk}) and the underlying theoretical support for the method can be found in Villadsen and Michelsen [1978] who also provides subroutine listings that used in this study. The boundary condition for the interface (ξ_c) between bulk phase and enzyme layer is $\phi_{i,Mk}=\phi_{ei,1k}$ where M is the number of collocation points that corresponds to a particular Mth-order polynomial approximation. And the boundary conditions for the input part of reactor are $\phi_{i,jl}=1$ for j=1~M − 1 and $\phi_{ei,hl}=0$ for all h. Substituting the above relationships, Eqs. (22)-(24), into the diffusion equations and boundary conditions yields a set of first-order differential equations.

For bulk phase,

$$\frac{d\phi_{i,jk}}{d\theta} = -\alpha \sum_{l=1}^{N} A_{kl}\phi_{i,jl} + \beta_i \sum_{q=1}^{M} C_{jq}\phi_{i,qk}, \quad j=2\text{~}M-1,\ k=2\text{~}N \qquad (25)$$

For enzyme layer

$$\frac{d\phi_{ei,hk}}{d\theta} = -\gamma_i \sum_{s=1}^{L} E_{hs}\,\phi_{ei,sk} + \Gamma_i, \quad h=2\text{~}L-1,\ k=2\text{~}N \qquad (26)$$

And, for boundary conditions

B.C.1: $\sum_{p=1}^{M} B_{1p}\phi_{i,pk} = 0,$ \qquad k=2~N \qquad (27)

B.C.2: $\sum_{r=1}^{L} D_{Lr}\phi_{i,rk} = 0,$ \qquad k=2~N \qquad (28)

B.C.3: $\sum_{p=1}^{M} B_{Mp}\phi_{i,pk} = \eta_i \sum_{r=1}^{L} D_{1r}\phi_{ei,rk},$ \qquad k=1~N \qquad (29)

that are easily integrated by an explicit Runge-Kutta type method [Maron, 1982] with the initial conditions $\phi_{i,jk}(0)=0$ and $\phi_{ei,hk}(0)=0$.

3. Parameter Estimation

Under the conditions where the rate constants of enzyme reaction are known and the diffusion coefficients in the bulk phase can be estimated a priori, the parameter to work with is D_{ei}. The diffusion coefficients of acetic acid in bulk phase is estimated as 1.3×10^{-5} cm^2/sec using the experimental data and correlation to compensate the temperature effect described by Perry and Green [1984]. The diffusion coefficients of acetylthiocholin iodide and paraoxon are calculated as 5.92×10^{-6} cm^2/sec and 6.07×10^{-6} cm^2/sec by Eq. (30) [Tyrrell and Harris, 1984] using the diffusivity of acetic acid and molecular weight (MW).

$$\frac{D_1}{D_2} = \sqrt{\frac{MW_2}{MW_1}} \qquad (30)$$

The solutions to Eqs. (25)-(29) depend on the choice of L, M, N and the polynomial used for the basic functions. The polynomial used in all numerical approximations is characterized by the weighting factor $\zeta^{1/2}(1-\zeta)$ over the interval $0<\zeta<1$ and $\xi^{1/2}(1-\xi)$ over the interval $0<\xi<1$. N=6 and M=4 for the bulk phase and L=3 for the enzyme layer are chosen as the number of collocation points, which represent a compromise between extreme accuracy and computational speed.

The experimental data, C_i vs. θ, are compared to the model predictions by choosing a diffusion coefficient of acetic acid in enzyme layer giving a best fit of the model to the data. During the computation, the diffusion coefficients of acetylthiocholin iodide and paraoxon are determined using the Eq. (30). A nonlinear parameter estimation package, NONLIN, is used [Metzler et al., 1974] that uses a weighting factor for the residuals, proportional to ϕ^{-2} so that the information near steady state condition is highlightened.

RESULTS AND DISCUSSION

1. Kinetics

The suggested inhibition kinetics was plotted with experimental data as shown in Fig. 4. The double reciprocal plots showed that the proposed kinetics was in a good agreement with the experimental data for the inhibitor concentration varied from 0 to 2 ppm (correlation coefficient : 0.96, 0.94, 0.94 for 0, 1, 2
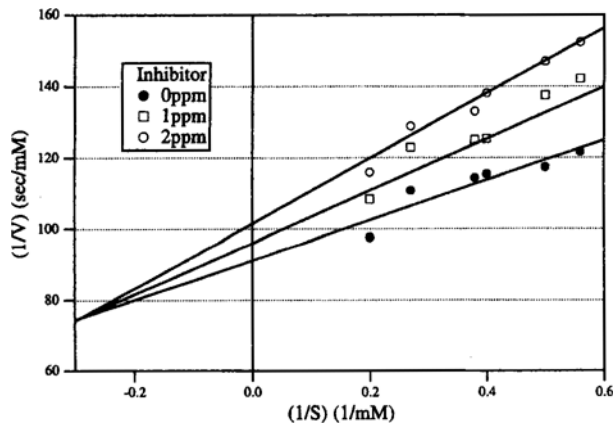
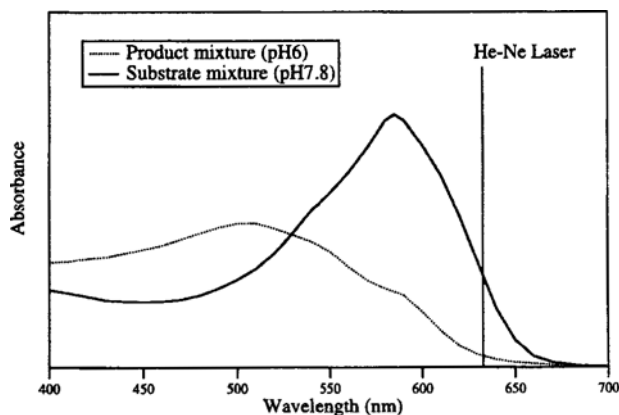Fig. 4. The reciprocal plot of experimental data for AChE reaction.

Fig. 6. Typical reference and indicator signal of sensor.

Fig. 5. The absorption spectra of substrate mixture and product mixture with litmus.
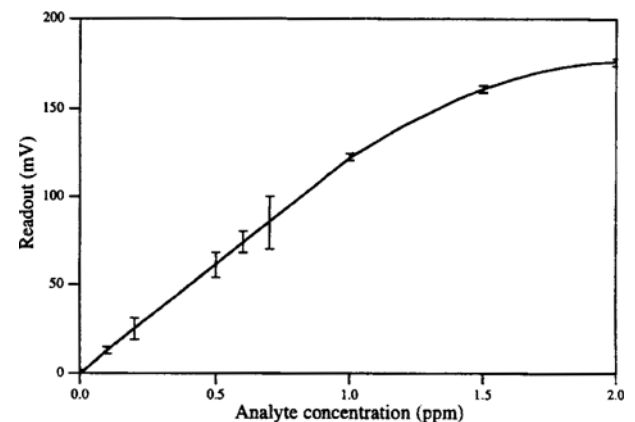
Fig. 7. Experimental (bar) and theoretical (line) result for the sensor signal.

ppm of analyte concentration, respectively). Fig. 4 showed that both K'_m and V'_{max} depend on the concentration of inhibitor. The proposed irreversible inhibition kinetics could describe the inhibition of organophosphorus compounds on AChE and thus should be utilized for the model of tubular enzyme reactor. The calculated kinetic constants were $V_{max}=1.1\times10^{-2}$ mMsec^{-1}, $k_m=$ 6.25×10^{-1} mM, $k_2=1.55\times10^{-2}$ sec^{-1} and $k_I=0.151$ mM.

2. Detection Principle

The acetylcholinestrase converted the acetylthiocholin iodide into acetic acid and thiocholin. The selection of dye was done based on the absorption spectra to 633 nm line of He-Ne laser and the transmissivity of fiber. The blue color of litmus dye was changed to the red color by the pH decrease due to the formation of acetic acid. The difference of absorption at 633 nm by enzyme reaction represented the product formation as shown in Fig. 5. As the inhibitor introduced, the decrease of the absorption difference was occurred due to the inhibition of inhibitor on the acetylcholinesterase, which was proportional to inhibitor concentration.

3. Sensor Signal Analysis

The transmittance via optical fiber was measured at the input and output parts of the tubular enzyme reactor as the reference and indicator signal, respectively, as shown in Fig. 6. When the substrate solution entered into the input part of tube, its transmittance was measured as the reference signal, which was
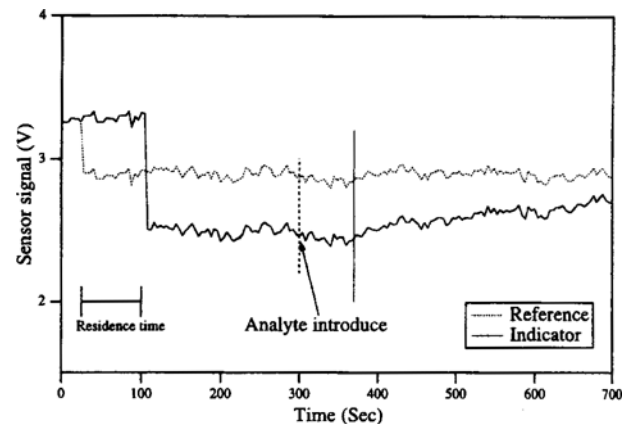
not varied due to enzyme reaction but fluctuated presumably due to the external light variation. When the flow was reached to the indicator probe, transmittance was reduced by the product formation. As the inhibitor was entered into the flow system with substrate solution, the product formation was reduced because immobilized enzyme was inactivated. Consequently, the indicator signal increased proportionally to the reduced amounts of product by inhibition of Paraoxon while the reference signal was not changed, and then which was modulated by Eq. (1) as the corrected sensor signal. The residence time was determined by the detection of the time interval between the reference signal drop and the indicator signal drop.

Fig. 7 represented that the corrected sensor signal was linearly proportional to Paraoxon concentration up to 1.0 ppm with a response time of 5 minutes experimentally. The model results were shown as the solid curves in Fig. 7. The experimental values in the model calculation were as follows; flow velocity= 0.8 mm/sec: reactor radius=3 mm: thickness of enzyme layer= 0.5 mm. Simulation results showed the experimental data fairly accurately at given operating condition. From the experimental data, the effective diffusivity of acetic acid in enzyme layer was estimated as 1.04×10^{-5} cm^2/sec. The order of estimated diffusivities was reasonable compared with the diffusivity of acetic acid in water calculated previously (1.3×10^{-5} cm^2/sec). Since the gel was constructed with viscous alginate, the effective diffusivity

of acetic acid is less than the diffusivity in water [Westrin and Axelsson, 1991]. The diffusion coefficients of acetylthiocholin iodide and paraoxon are calculated as 4.73×10^{-6} cm^2/sec and 4.86×10^{-6} cm^2/sec by Eq. (30) [Tyrrell and Harris, 1984]. The model was able to predict the upper limit of detection about 1.2 ppm of inhibitor concentration and the nonlinearity of sensor signal due to the saturation of enzyme reaction. To avoid the non-linear signal, the enzyme amount loaded should be increased.

4. Simulation to Investigate the Effects of Design and Operating Parameters

To analyze the transient response of sensor signal, the profile of enzyme activity inside the tubular enzyme reactor as the time course was calculated using the model. As the 2 ppm of paraoxon was flowed in, the amount of an inactivated enzyme was increased as the time course in Fig. 8(a). And it was different at each local position of enzyme layer inside the tubular enzyme reactor. At each local position, the amount of active enzyme tended to decrease with time by the paraoxon. But inactivated rate of enzyme was different in each local position along the reactor length because it was based on paraoxon concentration and inhibition time at each local position. Though the amount of active enzyme in the input part of tubular enzyme reactor disappeared rapidly within 180 sec after paraoxon flowed in, the one in the output part of tubular reactor was decreased slowly and was fully deactivated after 420 sec. The

result suggested that signal analysis should be done within 420 sec after the inhibitor was flowed into the tubular enzyme reactor.

In Fig. 8(b), the product concentration profile was calculated on the various analyte concentration using the model. In the absence of analyte, the product concentration was increased and reached to the steady concentration. Once the analyte was introduced into the reactor, the product were reduced rapidly due to an inactivation of immobilized enzyme after the residence time. The reduced amount of product concentration was increased as the analyte concentration was increased. Though the analyte concentration was sufficient to inactivate all amount of the enzyme, the product did not spontaneously reach the absolute zero concentration instantaneously. Because the product in the immobilized enzyme phase was diffused from the enzyme layer into the bulk phase with the lower velocity than that in bulk phase, it remained in the effluent after the inactivation of all enzymes.

To investigate the linear range of sensor signal, the effect of amount of immobilized enzyme on sensor signal was simulated using the model (Fig. 9). The more amount of immobilized enzyme was loaded in gel layer, the wider linear range for analytical detection was obtained. The optimum amount of enzyme loaded was 80 μg for the linear analytical range up to 2 ppm of inhibitor concentration as Korean 2nd effluent standard [Choi
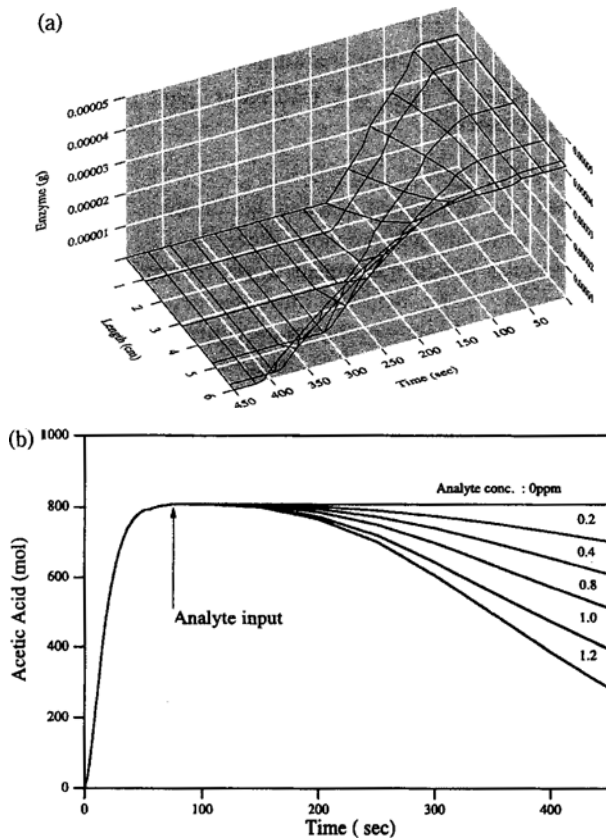

Fig. 8. (a) The simulation result of enzyme concentration in the reactor. (b) The simulation result of the transient response of product concentration for the effect of analyte concentration.
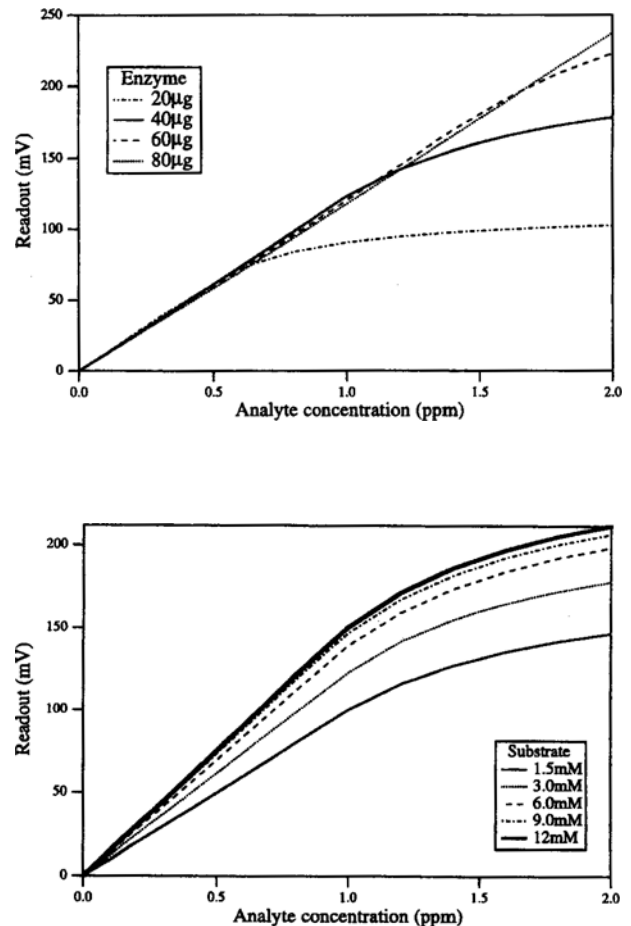

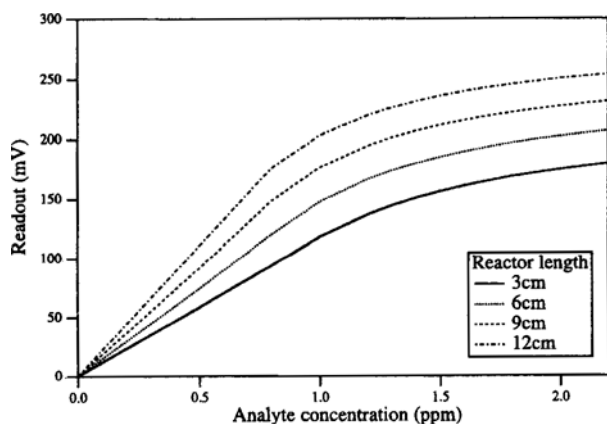Fig. 10. The simulation result of effect of the substrate concentration.

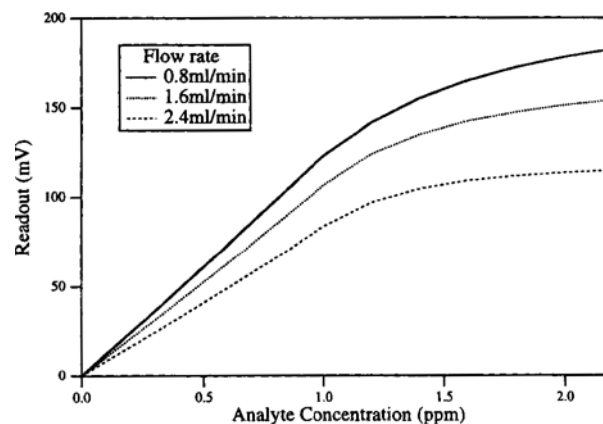**Fig. 11. The simulation result of effect of the reactor length.**

Fig. 12. The simulation result of effect of the flow velocity.

and Cho, 1990]. To optimize the substrate concentration, the effect of amount of substrate concentration on sensor signal was simulated in Fig. 10. Though the linear analytical range was not affected by the analyte concentration, the magnitude of readout signal was increased until reaction rate was maximized on substrate concentration. However, as substrate concentration was increased, the increment of sensor readout was decreased. Based on the extent of increment magnitude of readout signal, the optimum concentration of substrate could be suggested as 6 mM to increase the enzyme reaction rate economically and then to enlarge the readout signal.

Fig. 11 shows that the magnitude of the readout signal was enlarged as the reactor length was increased with the constant enzyme amount loaded. As the reactor length was increased, the residence time of substrate was increased and more amount of substrate was reacted with enzymes. Though the magnitude of a readout signal was enlarged as the reactor length was increased, the linear analytical range on the sample concentration was reduced. The reason might be that the volumetric concentration of enzyme in alginate gel was decreased since the surface area of enzyme layer contacted with analyte was increased. The optimum reactor length should be then decided by considering the linear analytical range needed, response time and magnitude of readout signal. With the constant enzyme amount loaded, the effect of substrate flow velocity on the sensor signal was simulated using the model in Fig. 12. The magnitude of readout signal was reduced as the flow rate was increased since the residence time was decreased. But the linear analytical range would not be varied because the inactivation rate of the enzyme was fast enough not to be affected by the decrease of residence time. As the residence time was decreased, the sensitivity of sensor signal was decreased.

CONCLUSIONS

The proposed fiber-optic biosensor can detect organophosphorus compounds with wide linear range and high sensitivity. The reaction part of the sensor consisted of a silicon tube containing a coordinated set of enzymes entrapped on the inner surface. Inhibition of organophosphorus compounds on AChE could be described by the proposed irreversible inhibition kinetics. Reasonable response time of about 5 minutes and linear analyt-

ical range of 0-1.0 ppm for the organophosphorus compounds were obtained. The proposed model for the tubular biosensor could predict the sensor signal for the various concentration of organophosphorus compounds (0-2 ppm). Based on the simulation for the transient response of sensor using the model, signal analysis should be done within 420 sec after the inhibitor injection. The optimum amount enzyme loaded was about 80 μg based on the model simulation to get the linear signal up to 2 ppm of inhibitor concentration and the optimum concentration of substrate was about 6 mM to increase the enzyme reaction rate economically and enlarge the readout signal. The magnitude of the readout signal was enlarged as the reactor length was increased but that was decreased as the flow rate was increased based on the simulation results.

NOMENCLATURE

A_{kl} : discretization elements for the derivation
B_{jp} : discretization elements for the derivation
C_{jq} : discretization elements for the derivation
C_i : concentration of i component in the bulk phase [M]
C_{ei} : concentration of i component in the enzyme phase [M]
C_{io} : input concentration of i component [M]
D_{jr} : discretization elements for the derivation
D : diffusion coefficient in the bulk phase [cm²/sec]
D_e : diffusion coefficient in the enzyme phase [cm²/sec]
E_{js} : discretization elements for the derivation
K_H : parameter combination
k_i : reaction rate constants
K_m : saturation constant
K'_m : modified saturation constant
V_{max} : maximum velocity of enzyme
V'_{max} : modified maximum velocity of enzyme
v : the flow rate of substrate [cm/sec]
V : the reaction rate
x : axial coordinate
y_c^+ : maginally lower than the interface position (y_c) [cm]
y_c^- : maginally high than the interface position (y_c) [cm]
t : time [sec]
y : radial coordinate
y_c : reactor radius to the interface between bulk phase and enzyme phase [cm]

y_o : reactor radius to the wall [cm]

Z   : reactor length

Greek Letters

α : dimensionless parameter [$=v\bar{t}/L$]

β : dimensionless parameter [$=D_i\bar{t}/y_o^2$]

γ : dimensionless parameter [$=D_{ei}\bar{t}/y_o^2$]

θ : dimensionless time [$=t/\bar{t}$]

ζ : dimensionless longitudinal coordinate [$=z/L$]

ξ : dimensionless radial coordinate [$=y/y_o$]

ω : dimensionless maximum velocity [$=V'_{max} C_{io}/\bar{t}$]

Γ_i : dimensionless reaction rate [$=V_i C_{io}/\bar{t}$]

κ : dimensionless saturation constant [$=k'_m/C_{1o}$]

η_i : effective diffusion coefficient [$=D_{ei}/D_i$]

ϕ : dimensionless concentration [C/C_o]

ϑ : sensor signal

ϑ' : corrected sensor signal modified by Eq. (1)

Superscripts and Subscripts

e   : enzyme phase

i   : component i

L   : number of collocation point to the radial direction within the enzyme (=3)

M   : number of collocation point to the radial direction within the bulk (=4)

N   : number of collocation point to the longitudinal direction (=6)

o   : initial concentration

rxn   : enzyme reaction period without the inhibitor

ACKNOWLEDGMENT

REFERENCES

Abdel-Latif, M. S. and Guidbault, G. G., "Fiber Optic-Based Biosensors Utilizing Immobilized Enzyme Systems", Biosensor Technology: Fundamentals and Applications, Buck, R. P., Hatfield, W. E., Umana, M. and Bowden, E. F., eds., Marcel Dekker, New York, 1990.

Alfthan, K., Kenttamaa, H. and Zukale, T., "Characterization and Semiquantitative Estimation of Organophosphorus Compounds Based on Inhibition of Cholinesterases", *Analytica Chimica Acta*, **217**, 43 (1989).

Carome, E. F., Coghlan, G. A., Sukenik, C. N. and Zull, J. E., "Fiber Optic Evanescent Wave Sensing of Antigen-Antibody Binding", *Sensors and Actuators B*, **13-14**, 732 (1993).

Choi, U. S and Cho, K. M., "Environmental Engineering", Ch-

eongmungak, Seoul, 1990.

Dumschat, C., Muller, H., Stein, K. and Schwedt, G., "Pesticide-Sensitive ISFET Based on Enzyme Inhibition", *Analytica Chimica Acta*, **252**, 7 (1991).

Klaimer, S. M., Thomas, J. R. and Franels, J. C., "Fiber-Optic Chemical Sensors Offer a Realistic Solution to Environmental Monitoring Needs", *Sensors and Actuators B*, **11**, 81 (1993).

Leon-Gonzalez, M. E. and Townshend, A., "Flow-Injection Determination of Paraoxon by Inhibition of Immobilized Acetylcholinesterase", *Analytica Chimica Acta*, **236**, 267 (1990).

Maron, M. J., "Numerical Analysis; A Practical Approach", Macmillan, New York, 1982.

Metzler, C. M., Elfring, G. L. and McEwen, A. J., "A Package of Computer Programs for Pharmacokinetic Modeling", *Biometrics*, **30**, 562 (1974).

Perry, R. H. and Green, D., "Perry's Chemical Engineering's Handbook", McGraw-Hill, New York, 1984.

Skladal, P., "Determination of Organophosphate and Carbamate Pesticides Using a Cobalt Phthalocyanine Modified Carbon Paste Electrode and a Cholinesterase Enzyme Membrane", *Analytica Chimica Acta*, **252**, 11 (1991).

Takruni, I. A., Almuaibed, A. M. and Townshend, A., "Flow-Injection Study of Inhibition and Reactivation of Immobilized Acetylcholinesterase: Determination of the Pesticides Paraoxon and Carbamoylcholin", *Analytica Chimica Acta*, **282**, 307 (1993).

Trettnak, W., Hofer, M. and Wolfbeis, O. S., "Applications of Optochemical Sensors for Measuring Environmental and Biochemical Quantities", Sensors, Vol. 3, Gopel, W., Hesse, J. and Zemel, J. N., eds.,VCH, New York, 1991.

Trettnak, W., Reininger, F., Zinterl, E. and Wolfbeis, O. S., "Fiber-Optic Remote Detection of Pesticides and Related Inhibitors of the Enzyme Acetylcholineesterase", *Sensors and Actuators B*, **11**, 87 (1993).

Tyrrell, H. I. V. and Harris, K. R., "Diffusion on Liquids", Butterworths, London, 1984.

Villadsen, J. and Michelsen, M. L., "Solution of Differential Equation Models by Polynomial Approximation", Prentice-Hall, Englewood Cliffs, 1978.

Wittmann, C. and Schmid, R. D., "Application of an Automated Quasi-Continuous Immuno Flow Injection System to the Analysis of Pesticide Residues in Environmental Water Samples", *Sensors and Actuators B*, **15-16**, 119 (1993).

Westrin, B. A. and Axelsson, A., "Diffusion in Gels Containing Immobilized Cells; A Critical Review", *Biotech. Bioeng.*, **38**, 439 (1991).

Wolfbeis, O. S. and Koller, E., "Fiber Optic Detection of Pesticides in Drinking Water", Biosensors Application in Medicine, Environmental Protection and Process Control, Schmid, R. D. and Scheller, F., eds., GBF, New York, 1989.